Visualization of polyethylene fibers surface restructuring induced by oxygen plasma

R. INTRATER
Space Environment Division, Soreq NRC, Yavne 81800, Israel; Department of Chemistry, Technion-Israel Institute of Technology, Haifa, 32000 Israel

A. HOFFMAN
Department of Chemistry, Technion-Israel Institute of Technology, Haifa, 32000 Israel

G. LEMPERT, I. GOUZMAN
Space Environment Division, Soreq NRC, Yavne 81800, Israel

Y. COHEN
Department of Chemical Engineering, Technion-Israel Institute of Technology, Haifa, 32000 Israel

E. GROSSMAN*
Space Environment Division, Soreq NRC, Yavne 81800, Israel
E-mail: eitan@soreq.gov.il

Published online: 1 November 2005

Considerable research has been undertaken on the effect of the oxygen plasma treatment on the surface of Ultra High Molecular Weight Polyethylene (UHMWPE) fibers [1–3]. Gao *et al*. [2] have characterized the chemical and physical changes of the fibers caused by plasma oxygen treatment. Plasma treatment produced a dramatic change in surface morphology and highly developed structure replaced the long straight fibrils. Gao [2] attributed this structure formation to molecular chain degradation on fiber surfaces as a result of plasma etching. The surface modification of a polyethylene fiber treated in oxygen plasma was investigated also by Woods and Ward [3]. They studied the effect of the surface oxidation on the interlaminar shear strength (ILSS) of polyethylene fiber/epoxy resin composites. Their conclusion was that surface oxidation makes a major contribution to the initial increase in ILSS for short treatment times.

In this paper we report, for the first time, the direct visualization of the surface restructuring, at the nano-scale level, of UHMWPE fibers into oriented-row structures at ambient temperature. These row-structures were induced by simultaneous exposure of the fibers to the oxygen plasma afterglow together with RF plasma-originated UV radiation, in a single-stage process.

The polyethylene ultra strong fibers exhibit a well-defined aggregate structure. They are made of micro fibrils (100–150 nm in diameter), which themselves are composed of nanofibrils (5 nm in diameter) as illustrated schematically in Fig. 1. The structure of these extended chains fibers was characterized with the aid of TEM [4–6], wide angle and small angle X-ray diffraction [6], and AFM [7, 8]. The structure of the fibers was also investigated using SEM and TEM [9] following chemical etching [10]. The microfibrils have a finite length of about 1–2 μm [11]. The longitudinal structure of the nanofibrils was found to be inhomogeneous, containing regions of different density that could be attributed to domains containing high concentration of crystal defects. These "amorphous" domains are covalently bonded to the adjacent nearly perfect rod-like crystalline domains ~200 nm long [11]. Fig. 1 is a schematic illustration of the ultra-strong UHMWPE fiber structure, in which high strength and high modulus crystals are covalently bonded to the surrounding "amorphous" matrix [11–13]. The structure in Fig. 1 is based on small angle and wide angle X-ray diffraction, electron microscopy, NMR, and micro-Raman studies [12]. This model rationalizes the mechanical properties of ultra-strong UHMWPE fiber [14], including its outstanding damage tolerance and impact resistance [14].

In the present work, the initial unexposed sample material was 1 mm thick ultra-strong polyethylene fiber composite (manufactured by PolyEitan Composites Ltd.) [15]. The composite is fabricated by compaction of extended chain UHMWPE fibers under high pressure without any extraneous binder. Fiber bonding is due to a transition of a thin (few nm) surface layer to the more mobile state, retaining its high axial orientation [16]. The samples were

* Author to whom all correspondence should be addressed.

0022-2461
DOI: 10.1007/s10853-005-2733-x

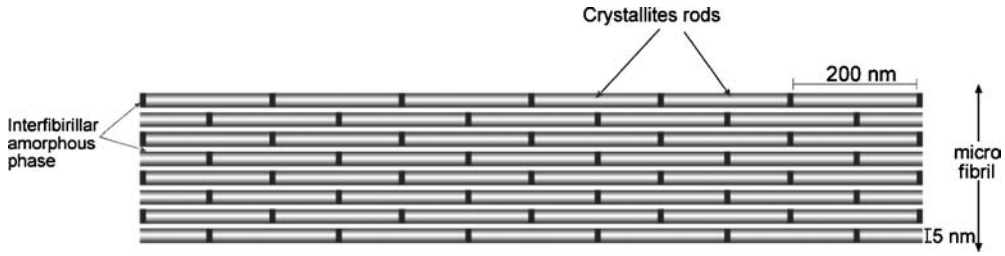

Figure 1 Schematic longitudinal view of ultra-strong polyethylene fiber structure [12].

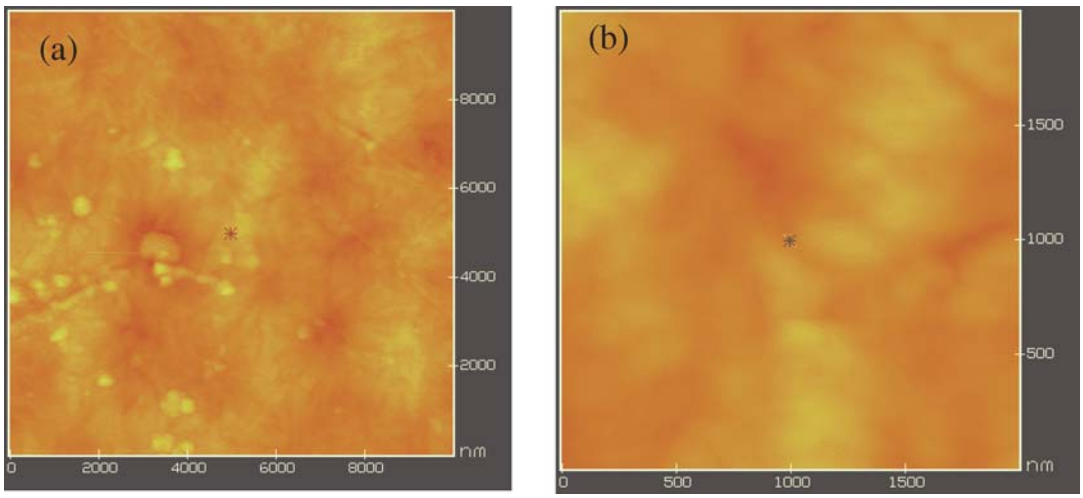

Figure 2 AFM images of ultra-strong (UHMWPE) fibers chemically etched: (a) Scan area 10×10 μm^2, (b) scan area 2×2 μm^2.The *Z* scale is 500 nm.

irradiated in the afterglow region of a high power (1200 W) RF plasma reactor (Litmas Model LB1200). The samples were located on a sample mounting stage, enabling exposure to controlled afterglow conditions. The samples were exposed to the full oxygen plasma afterglow flow, with and without UV radiation, generated by the plasma. The UV irradiating the sample could be effectively turned on and off by blocking or unblocking a MgF_2 window mounted directly between the plasma and the sample. The oxygen flux was maintained constant in both cases (MgF_2 window either blocked or unblocked). The reference sample was prepared by chemically etching of the composite material in permanganate solution [10]. The surface morphology of the samples was analyzed with the aid of an Atomic Force Microscope (AFM) in contact (DI NanoScopeII) and tapping (DI Multimode) modes. The chemical modifications were characterized using ATR-FTIR (Nicollet MAGNA-IR 550 series).

The effect of the exposure to oxygen RF plasma in the after glow together with UV radiation, as compared to exposure to oxygen alone, is illustrated in Figs 2–6. Figs 2–4 show AFM images of the composite polyethylene fiber

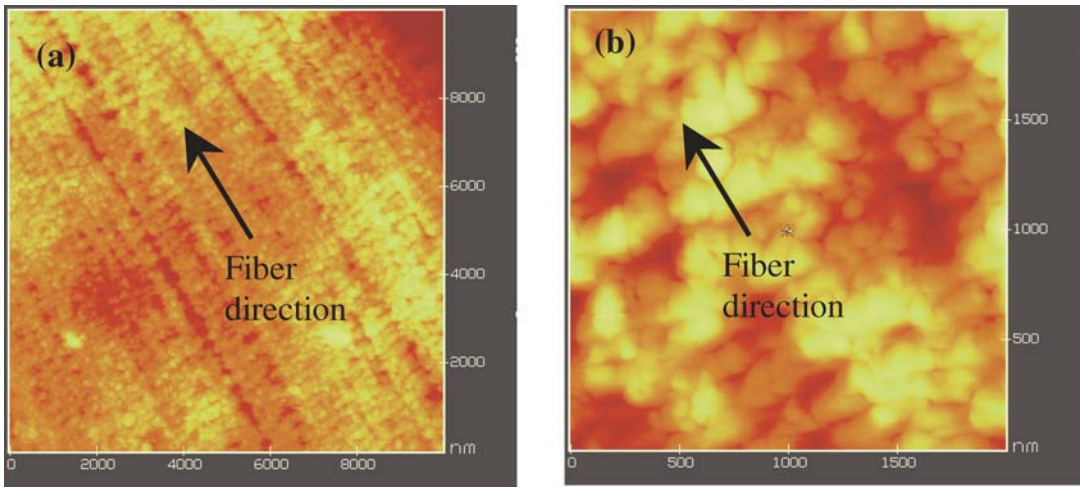

Figure 3 AFM images of ultra-strong (UHMWPE) fibers exposed to the oxygen RF plasma with no UV radiation: (a) Scan area 10×10 μm^2, (b) scan area 2×2 μm^2.The *Z* scale is 500 nm.

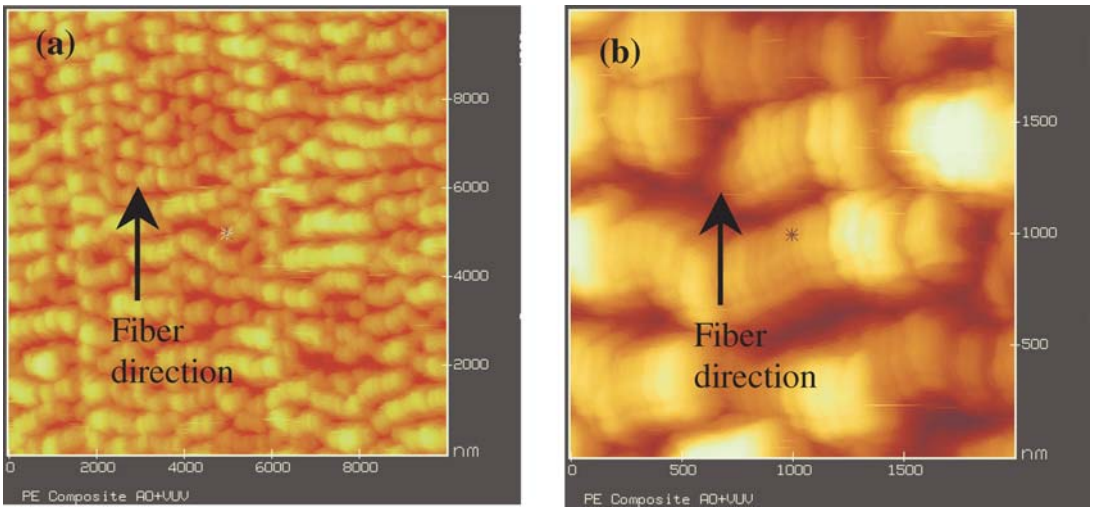

Figure 4 AFM contact images of ultra-strong (UHMWPE) fibers exposed to the oxygen RF plasma with UV radiation: (a) Scan area 10×10 μm^2, (b) scan area 2×2 μm^2.The Z scale is 500 nm.

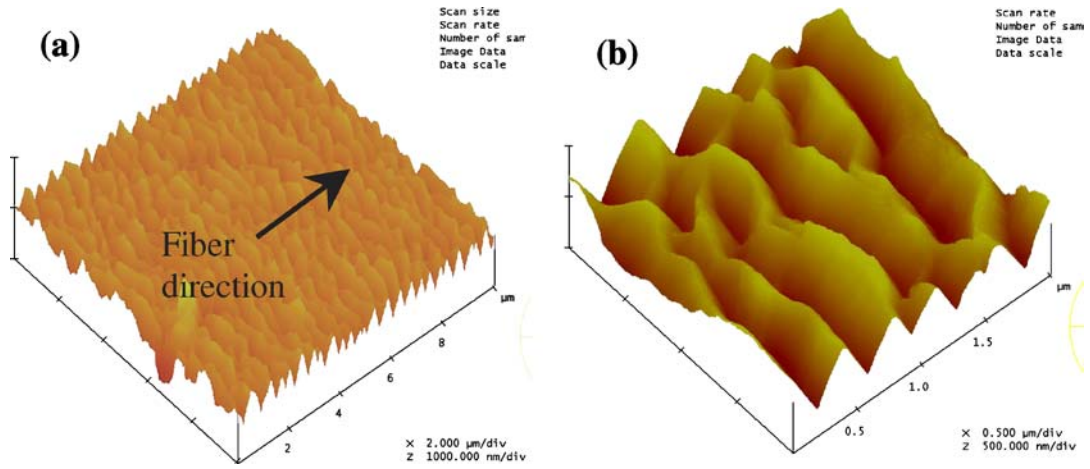

Figure 5 AFM tapping images of ultra-strong (UHMWPE) fibers exposed to the oxygen RF plasma with UV radiation: (a) Scan area 10×10 μm^2, (b) scan area 2×2 μm^2.The Z scale is 500 nm.

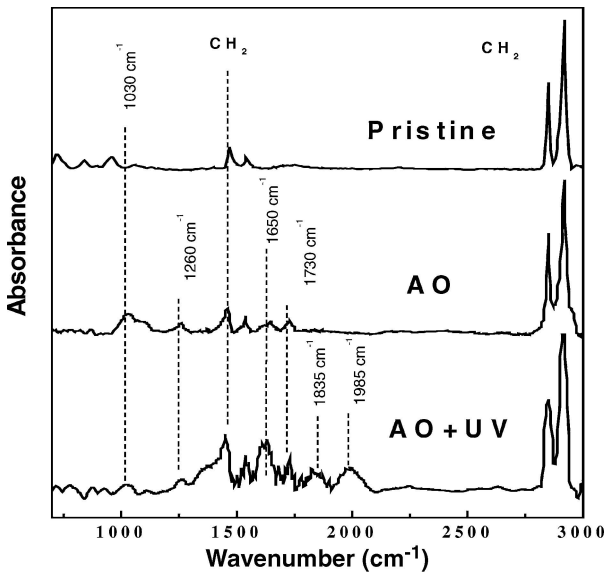

Figure 6 ATR-FTIR spectra of composite polyethylene (PolyEitan): pristine exposed to AO and to AO + VUV.

surface obtained in contact mode and Fig. 5 shows image obtained in tapping mode. Fig. 2a and b show the reference surface after chemical etching. In these images, no ordered patterns were observed and the fiber surface was relatively smooth compared to the plasma etched surfaces. Fig. 3 shows the composite polyethylene fiber surface after exposure to oxygen RF plasma afterglow without UV radiation (further referred to as oxygen alone). In this image, the uniform etch of the surface revealed the oriented fibrillar structure of the polyethylene fiber. The higher resolution image (Fig. 3b) shows typical morphology (carpet like) of an oxygen RF plasma etched polymer surface [17]. Fig. 4 shows AFM images of the composite polyethylene fiber surface after simultaneous exposure to the oxygen RF plasma and UV radiation. In Fig. 4a, the formation of an ordered narrow row-structure, perpendicular to the polyethylene fiber direction is observed. In Fig. 4b, it is seen that these row structures themselves have internal fine structure of parallel rod-like nanofibrils packed together perpendicular to the row direction. Fig. 5

is a 3D tapping mode AFM image of the sample after simultaneous exposure to the RF plasma afterglow and UV radiation. In Fig. 5a, the formation of an ordered narrow row-structure, perpendicular to the polyethylene fiber direction is also observed. Fig. 5b is higher resolution image and it shows the row structure as previously seen in the contact mode AFM image (Fig. 4). Fig. 6 shows the ATR-FTIR spectra of PolyEitan surfaces, respectively, before and after exposure to Atomic Oxygen (AO) flux alone and combined AO + VUV flux. Addition of UV to the AO resulted in a significant increase in the oxidative agents, indicating the depth effect of the UV radiation. The UV radiation creates radicals below the surface; the oxygen diffuses and reacts with these radicals. The result is higher total oxidative species as seen in the ATR-FTIR spectrum.

Such room-temperature surface patterning (Fig. 4) has not been previously reported for ultra-strong UHMWPE fibers to the best of our knowledge. It should be emphasized that according to the widely accepted ultra-strong UHMWPE fiber structure model [12] (see Fig. 1), the nanofibrils crystallites are not aligned; while the observed oxygen RF plasma exposed material reveals well aligned rod-like nanofibrils (Fig. 4b).

The image in Fig. 4b, shows a row structure with stripes of needle-like rods. This rearrangement is very similar to the classic row-nucleated lamellar structure [18]. The row nucleation structure is formed when a highly crystalline polymer-oriented chains recrystallizes under high stress at a temperature close to its melting point [18, 19]. The crystallization under stress leads to a segmental crystalline orientation perpendicular to the stress direction. The perpendicular orientation is considered as being the result of the folding of oriented chains leading to lamellae, aligned along the stress direction. In this study, a row structure was formed at ambient temperature with no external stress.

There are experimental results showing the tendency of polyethylene to spontaneously rearrange into ordered structures. It was found that when polyethylene melt crystallizes over polyethylene fiber, a well-defined region of row-nucleated matrix is formed in the absence of stress [20–23]. This is an experimental evidence that shows that the polyethylene fiber has strong ability to induce oriented crystal growth into row structures even from randomly distributed polyethylene chains under no stress. Another example is the formation of "shish kebab" crystals on top of an oriented extended chain backbone substrate [24]. On this oriented substrate, the lamellae grow in parallel to each other and perpendicular to the main direction.

A possible model explaining the UHMWPE fiber surface RT restructuring due to oxygen plasma exposure may be based on the preferential etching of the amorphous phase compared to the crystalline phase during the simultaneous oxygen RF plasma and UV irradiation [25]. The ultra-strong polyethylene fiber is composed of nano rod-like crystallites separated by amorphous domains [12] as described in Fig. 1. The energetic UV radiation (3–7 eV for 100–180 nm UV range) penetrates through this composite structure to a depth of ~100 nm [26–28], creating active sites on and below the surface. The atomic oxygen diffusion into the polymer is dictated by its structure. Sorption and diffusion take place exclusively in the amorphous regions, while the crystalline zones are impermeable barriers for the diffusion process [29, 30]. ATR-FTIR results indicate such oxygen diffusion and formation of oxidative species, such as demonstrated by the formation of a new band near 1980 cm^{-1}, possibly attributed to O=C–O–O–C=O groups. The restructuring might be therefore attributed to preferential etching of the amorphous domains resulting in rod-like crystallites surface-rich. It is anticipated that future results will provide improved insight and evaluation with regard to the formation mechanism of the surface row restructuring process.

The reconstruction of row-structures on top of an oriented polyethylene substrate at ambient temperatures could improve existing applications and suggest new opportunities. This new surface patterning might add mechanical keying effects in the adhesion of UHMWPE fiber to resins, thus increasing the average shear strength.

Acknowledgments

This work was partially supported by the Israeli Space Agency. The authors would like to thank Professor Y. Lifshitz for productive discussions.

References

1. S. I. MOON and J. JANG, *ibid.* **68** (1998) 1117.
2. S. GAO and Y. ZENG, *J. Appl. Polym. Sci.* **47** (1993) 2093.
3. D. W. WOODS and I. M. WARD, *Surf. Interf. Anal.* **20** (1993) 385.
4. S. S. SHEIKO, M. MOLLER, M. KUNZ and H. DECKMANN, *Acta Polym.* **47** (1996) 492.
5. A. SCHAPER, D. ZENRE, E. SCHULZ, R. HIRTL and M. TAEGE, *Phys. Stat. Sol. (A)* **116** (1989) 179.
6. D. HOFMANN and E. SCHULZ, *Polymer* **30** (1989) 1964.
7. A. WAWKUSCHESKI, H. K. CANTOW and S. N. MAGONOV, *Polym. Bull.* **32** (1994) 235.
8. W. HU, A. BURIN, J. S. LIN and B. WUNDERLICH, *Polym Sci. Part B: Polym. Phys.* **41** (2003) 403.
9. M. I. ABO EL-MAATY, R. H. OLLEY and D. C. BASSET, *J. Mater. Sci.* **34** (1999) 1975.
10. M. M. SHAHIN, R. H. OLLEY and M. J. BLISSET, *Polym. Sci. Part B: Polym. Phys.* **37** (1999) 2279.
11. S. KOVESH and D. C. PREVORSEK, *Int. J. Polym. Mater.* **30** (1995) 15.
12. D. C. PREVORSEK, *Trends Polym. Sci.* **3**(1) (1995) 4.
13. L. I. SLUTSKER, *J. Polym. Sci. Part B: Polym. Phys.* **25** (1987) 525.
14. D. C. PREVORSEK, H. B. CHIN and S. MUTHY, *J. Polym. Sci. Polym. Symp.* **75** (1993) 81.
15. D. M. REIN, L. VAYKHANSKY, R. L. KHALFIN, and Y. COHEN, *Polym. Adv. Technol.* **13** (2002) 1046.
16. D. M. REIN, L. SHAVIT, R. L. KHALFIN, Y. COHEN, A. TERRY and S. RASTOGI, *Polym. Sci. Part B: Polym. Phys.* **42** (2004) 53.
17. A. F. WHITAKER and B. Z. JANG, *J. Appl. Polym. Sci.* **48** (1993) 1341.
18. X. M. ZHANG, S. ELKAUN, A. AJJI, and M. A. HUNEAULT, *Polymer* **45** (2004) 217.

19. R. T. CHEN, C. K. SAW, M. G. JAMIESON, T. R. AVERSA and R. w. CALLAHAN, *J. Appl. Polym. Sci.* **53** (1994) 471.
20. H. TIANBAI and R. S. PORTER, *ibid.* **35** (1988) 1945.
21. M. I. ABO EL MAATY and D. C. BASSETT, *Polymer* **43** (2002) 6541.
22. *Idem.*, *J. Macromol. Sci. Phys.* **B42** (2003) 687.
23. D. ROLEL, E. YAVIN, E. WACHTEL and H. D. WAGNER, *Comp. Interf.* **1** (1993) 225.
24. J. K. HOBBS, A. D. L. HUMPHRIS and M. J. MILES, *Macromol.* **34** (2001) 5508.
25. R. INTRATER, G. LEMPERT, I. GOUZMAN, E. GROSSMAN, Y. COHEN, D. M. REIN, R. L. KHALFIN and A. HOFFMAN, *J. High Perform. Polym.* **16** (2004) 249.
26. M. R. ADAMS and A. GARTON, *Polym. Durabil.* **10** (1996) 139.
27. A. C. FOZZA, J. ROCK, KLEMBERG J. E. SAPIEHA, A. KRUSE, A. HOLLANDER, M. R. WERTHEIMER, *Nucl. Instr. Meth.* **B131** (1997) 205.
28. V. N. VASILETS, I. HIRATA, H. IWATA and Y. IKADA, *J. Polym. Sci.* **A36** (1998) 2215.
29. M. H. KLOPFFER and B. FLACONNECHE, *Oil Gas Sci. Technol.—Rev. IFP* **56** (2001) 223.
30. D. J. SEKELIK and J. POLYMER, *Polym. Sci.: Part B: Polym. Phys.* **37** (1999) 847.

Received 13 March
and accepted 1 June 2005